PRAMANA
— journal of
physics

Vol. 76, No. 6
June 2011
pp. 973–983

Influence of drying conditions on the optical and structural properties of sol–gel-derived ZnO nanocrystalline films

A PAKDEL and F E GHODSI*

Department of Physics, Faculty of Science, The University of Guilan, Namjoo Ave.,
P.O. Box 41335-1914, Rasht, Iran
*Corresponding author. E-mail: feghodsi@guilan.ac.ir

MS received 14 September 2010; revised 23 November 2010; accepted 12 January 2011

Abstract. Zinc oxide nanothin films were prepared on glass substrate by sol–gel dip-coating method using zinc acetate dihydrate, methanol, and monoethanolamine as precursor, solvent, and stabilizer, respectively. The relationship between drying conditions and the characteristics of ZnO nanocrystalline films (*c*-axis orientation, grain size, roughness and optical properties) was studied. The films were dried in an oven at different temperatures and by IR radiation. Then, the films were annealed at 500°C in a furnace. The chemical composition, transmission spectra, structure, and morphology of the samples were studied using infrared (IR) and UV–visible spectroscopy, X-ray diffraction (XRD), and atomic force microscopy (AFM), respectively. The XRD results show that the drying conditions affect the orientation of crystallization along the (0 0 2) plane. AFM images show that the thicknesses of the films decrease from 128 to 93 nm by changing the drying conditions. The photoluminescence (PL) of ZnO nanothin films shows the UV emission at near band edge and broad green radiation at about 465 nm wavelength.

Keywords. ZnO; nanocrystalline films; drying; sol–gel.

PACS Nos 78.20.Ci; 81.20.Fw; 78.66.Bz; 78.67.–n

1. Introduction

Recently, zinc oxide-based thin films are attracting much attention because of their many different applications in both microelectronic and optoelectronic devices. ZnO thin film is a wide band-gap semiconductor with a direct energy gap of about 3.27 eV. Consequently, ZnO thin films absorb UV radiation due to band-to-band transitions. In addition, it can be used as transparent conductive oxide (TCO) thin films, mainly in gas sensors [1, 2], solar cells [3], functional glasses, and liquid crystal displays. Many techniques have been employed for the deposition of high-quality ZnO thin films such as chemical vapour deposition (CVD), magnetron sputtering, and spray pyrolysis [4–6]. Magnetron sputtering is generally accepted as an optimum method for preparing ZnO-based films. However, magnetron sputtering requires a complex and expensive vacuum technique and has its distinct

challenges when it comes to large area coating and film deposition on substrates having a complex geometry. An alternative deposition technique that can easily overcome these issues is the sol–gel method. Zinc oxide can be produced in various phases such as wurtzite, zincblende, and rock salt. Theoretical calculations indicate that a fourth phase, simple cubic, may be possible at extremely high temperatures. But, this phase has yet to be experimentally observed [7]. Crystallization of zinc oxide in the wurtzite structure is a tetrahedrally coordinated structure with hexagonal lattice. Zinc oxide thin films can crystallize in different orientations as a function of deposition method, annealing temperature, substrate, etc. The most possible orientation is the (0 0 2) hexagonal wurtzite orientation. High-quality *c*-axis-oriented ZnO thin films are very useful in optoelectronic devices. In addition, the *c*-axis-oriented films have some applications such as shear wave transducer and SAW filters [8] and only films having the *c*-axis orientation show some photocurrent phenomena. Many researchers have prepared zinc oxide thin films using the sol–gel process [9–11]. Most authors have focussed their attention on the effect of annealing temperature on the crystallization and their optical properties, and have considered high temperatures for the drying cycle [12–14]. In our knowledge, there has not been any investigation on the effects of drying condition on the physical behaviour of ZnO films. It is well known that infrared dryer at 100–150°C temperature removes solvents and water. But, the role of infrared dryer for stabilizers such as monoethanolamine at these temperatures is not well known.

In this work, ZnO thin films were prepared using zinc acetate dihydrate, methanol, and monoethanolamine (MEA) as starting material, solvent, and stabilizer, respectively. Then, one of the films was exposed to IR radiation and the others were dried in an oven at different temperatures. We have observed that the drying condition of the dip-coated ZnO thin films affects the *c*-axis crystal orientation of the films, their structural and optical properties, strongly.

2. Experimental methods

In this work, ZnO thin films were prepared by sol–gel method and deposited on glass substrate by dip-coating technique. Zinc acetate dihydrate ($Zn(CH_3COO)_2{\cdot}2H_2O$, 99%, Merck) was first dissolved in methanol (CH_3OH, 99.8%, Romil) and stirred at room temperature. When the solution turned milky, a suitable amount of monoethanolamine (MEA, C_2H_7NO, 98%, Merck) was added to the solution. Then, the mixed solution was stirred at 40°C for 30 min, until it became clear and homogeneous. The clear solution was kept for 24 h at room temperature. The viscosity and pH of the solution were about 2.80 mPa·s and 7.7, respectively. The films were deposited on glass (Corning Inc. 2947) substrates by dip-coating technique with a withdraw speed of 8.5 cm min^{-1}. The coated substrates were dried at different temperatures (175, 200, 225 and 250°C) for 20 min in an oven after each dipping procedure. One of the samples dried by IR radiation for 20 min using a special short-wave infrared lamp (SICCATHERM OSRAM lamp with maximum radiation at a wavelength of about 1100 nm, intensity about 2.5 W/cm^2 and a temperature about 140°C over the sample) was equipped with a hyperbolic reflector. The intensity of beams was focussed on 1×3 $inch^2$ area of the sample by transmitting the beams through a slit. The temperature of the sample was determined by a digital thermometer. The coating procedure

was repeated three times for all samples in the same sol conditions. Then, the films were annealed in a furnace at 500°C for 30 min.

The crystalline phase and orientations of the films were determined by the PHILIPS 1840 X-ray diffractometer (Cu K_α radiation, $\lambda = 1.542$ Å) with an angle step of 0.2°. A CARY-100 UV-VIS spectrophotometer was used to determine the optical transmittance over the spectral range from 200 to 800 nm at normal incidence and at room temperature. The optical constants and thickness of the films were determined by pointwise unconstrained optimization approach (PUMA) using empirical transmittance spectra in the visible region [15–17]. The topography and surface roughness of the samples were investigated using atomic force microscope (AFM, Nano Surf 2006). The optical emission studies on the ZnO nanocrystalline films were carried out by photoluminescence (PL) spectroscopy using a JASCO FP-6200 spectrofluorometer. The IR spectra of the precursor sol and thin films heated at different conditions were measured by a SHIMADZU-FD-1 infrared spectrometer over the spectral range from 400 to 4000 cm^{-1} wave number.

3. Results and discussion

The IR transmittance spectra of the sol and films dried in an oven at 110, 175, 250, 300°C, and film dried by IR radiation are shown in figure 1. The films have been scraped off from NaCl substrate. The curve (a) indicates peaks of the sol. It can be easily observed that the broad band assigned to water and alcohol O–H vibrations are at ∼3350 cm^{-1}, and the peaks of asymmetric and symmetric stretching vibrations of C=O groups are at 1558

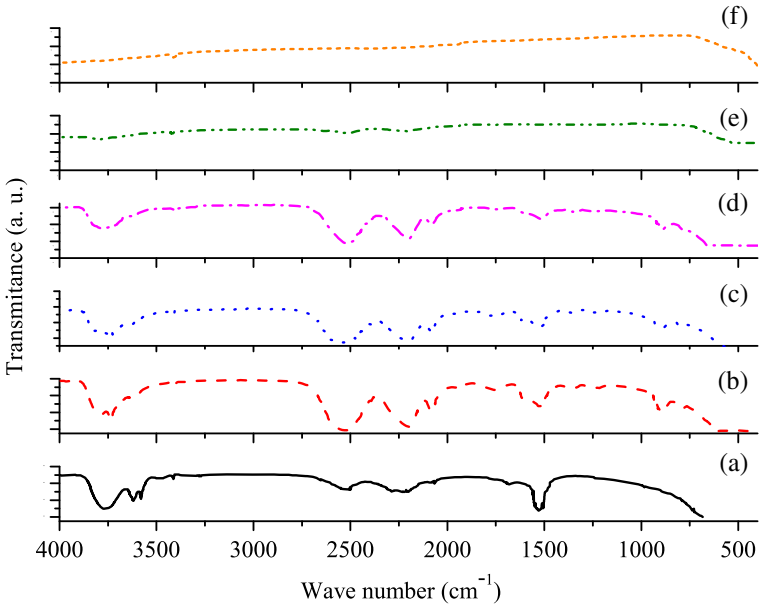

Figure 1. IR spectra of (**a**) precursor sol, (**b**)–(**f**) thin films dried at different conditions ((**b**) 110°C, (**c**) IR radiation, (**d**) 175°C, (**e**) 250°C and (**f**) 300°C) for 20 min.

and 1448 cm^{-1}. It is considered that the peaks near 2933 and 2868 cm^{-1} are due to the asymmetric and symmetric C–H bonds in MEA or due to the reaction between monoacetate and MEA [18–20]. The presence of NH group is responsible for the occurrence of a small peak near 3251 cm^{-1}. We found that when the drying temperature was above 300°C, the vapourization of the solvents and the thermal decomposition of zinc acetate occurred abruptly, and it simultaneously distributed the preferred crystal growth (XRD results). The sample dried at 110°C had no sensible results to offer.

Figure 2 shows XRD patterns of ZnO nanocrystalline films dried at different temperatures and by IR radiation followed by annealing at 500°C for 30 min. For films dried at 175°C and by IR radiation, the main peak is weak. The intensity of the (0 0 2) diffraction peak increases strongly with increasing drying temperature up to 250°C which indicates that the film dried at 225°C was strongly *c*-axis-oriented and the diffraction peaks reduced with increasing drying temperature above 225°C. It indicates that the grains grow with preferred orientation along the (0 0 2) plane [21]. For ZnO nanocrystalline film dried at 225°C, the highly preferred orientation is along (0 0 2) plane. The film dried at 225°C has a maximum (0 0 2) peak. The stoichiometry of the nanocrystalline film dried up to 225°C is improved and the defect number decreases. In the study related with *c*-axis growth from zinc acetate solution, the solvent, drying temperature, and the annealing temperature [22] affect the crystallization of ZnO thin films. By using 1-butanol or 2-methoxyethanol with high boiling temperature, the ZnO thin films have a highly *c*-axis-oriented (0 0 2) peak and two weak (1 0 0) and (1 0 1) peaks [19]. Since the boiling points of the solvents, methanol and MEA, are 64 and 170°C, respectively, drying temperatures as high as 175 and 200°C must be required for these solvents to vapourize completely. The thermal decomposition temperature of zinc acetate is 240°C and the crystallization of the ZnO film prepared from

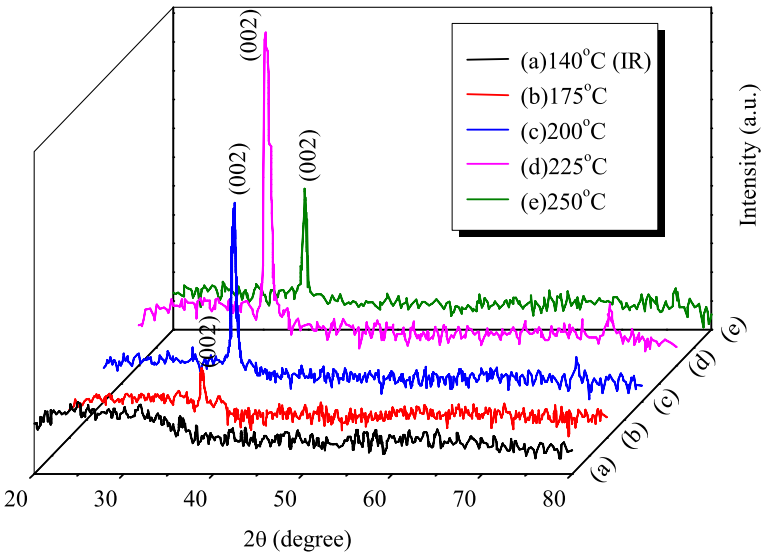

Figure 2. XRD pattern of ZnO nanocrystalline films dried at different temperatures and by IR radiation with annealing at 500°C.

zinc acetate–methanol–MEA solution begins at about 240°C. When the drying temperature is more than 240°C, the vapourization of the solvents and the thermal decomposition of zinc acetate will occur abruptly and simultaneously with the crystallization, disturbing the preferred crystal growth. On the other hand, when the drying temperature is too low (below 175°C), the complete vapourization and the thermal decomposition of zinc acetate do not occur at the drying step. Then, abrupt solvent vapourization and acetate decomposition occur at an annealing step, which disturbs the preferred crystal growth. Thus, the drying temperature is an important factor for preparing ZnO films with a preferred orientation along *c*-axis, affecting the solvent vapourization, zinc acetate decomposition and ZnO crystal growth [22–24].

Figure 3 shows the optical transmittance of the ZnO nanocrystalline films dried at different temperatures from 175 to 250°C and IR radiation for 20 min and annealed at 500°C for 30 min. The scatters and lines in figure 3 show the transmittances estimated with the PUMA and experimental data, respectively. The optical transmittance at 550 nm wavelength was changed from 61 to 92%. The optical transmittance was above 92% for the ZnO nanocrystalline film dried at 225°C and about 61% for the film dried by IR radiation. The optical transmittance increases with increasing drying temperature from 175 to 225°C and then decreases at 250°C. The films dried at 200 and 225°C were found to be transparent in the visible range with a sharp absorption edge at wavelengths of about 375 nm, which is very close to the intrinsic band gap of the ZnO films (3.3 eV). However, the transmittance of the films dried at 175°C and the films dried by IR radiation decreases and sharp absorption edges of these samples shift toward long wavelengths due to increasing optical scattering for these samples. On the other hand, the optical transmittance increases as being highly

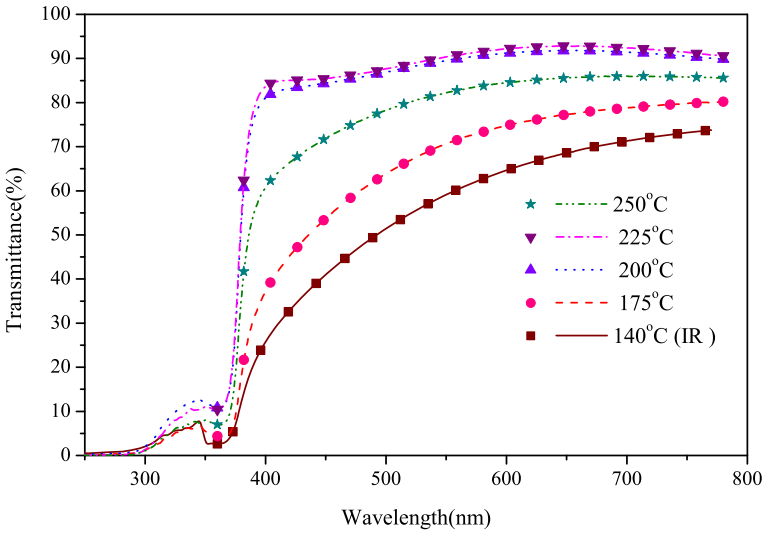

Figure 3. Optical transmittance spectra of ZnO nanocrystalline films dried at different temperatures and by IR radiation with annealing at 500°C. (line) experimental, (scatter) estimated with PUMA.

preferred oriented to c-axis and decreases as the film thickness increases. By increasing the drying temperature from 140 (IR radiation) to 250°C, the film thickness decreases from 128 to 93 nm. We expect the transmittance to increase by increasing drying temperature to 250°C and decreasing thickness to about 93 nm. This behaviour occurred for drying temperature up to 225°C. However, the transmittance decreases for 250°C drying temperature. It may be due to the decrease of the orientation along c-axis (as can be seen from XRD result for 250°C drying temperature). Thus the transmittance decreases and consequently much light is dispersed in grain boundary. Thus, the ZnO nanocrystalline film dried at 225°C temperature shows high orientation along the c-axis and high transmittance due to decrease of the optical scattering.

Figure 4 shows the spectral dependence of the refractive indices of ZnO nanocrystalline films dried at different conditions. The scatters and lines in figure 4 show the refractive indices estimated with PUMA and Cauchy dispersion relationship, respectively. It can be seen that the refractive index decreases with increasing drying temperature with an exception for the sample dried at 250°C, and its optical scattering is high due to the densification of the films as discussed. The scattered radiations become remarkable due to the surface roughness [25]. Figure 5 shows the drying temperature dependence of the extinction coefficients of the ZnO nanocrystalline films. The scatters and lines in figure 5 show the extinction coefficients estimated with PUMA and Cauchy dispersion relationship, respectively. It is obvious that the extinction coefficients change with respect to drying conditions as the refractive index changes. When densification of the film increases, the optical scattering of the sample increases and more optical radiation can be absorbed.

Figure 6 shows $(\alpha h\upsilon)^2$ vs. $h\upsilon$ for the ZnO nanocrystalline films at different drying temperatures. The optical band gap (E_g) can be obtained by plotting $(\alpha h\upsilon)^2$ vs. $h\upsilon$ and

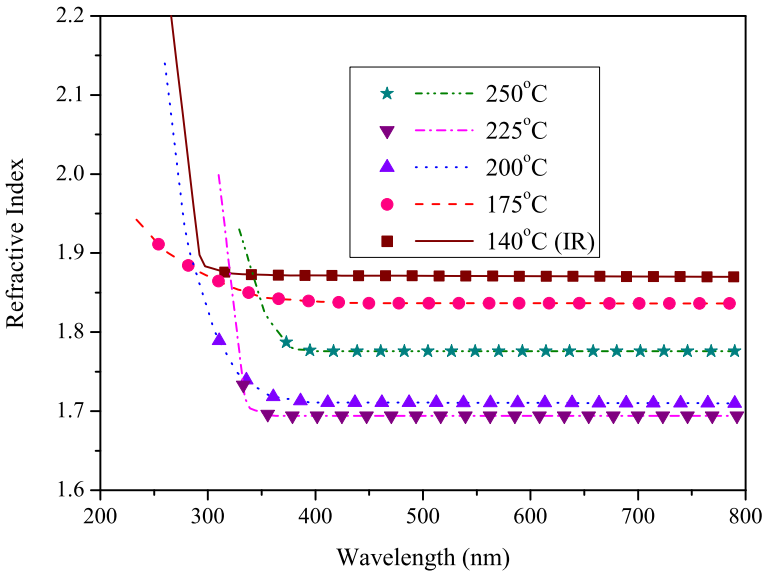

Figure 4. The refractive indices of the ZnO nanocrystalline films dried at different temperatures and by IR radiation. (line) Cauchy fitting, (scatter) estimated with PUMA.

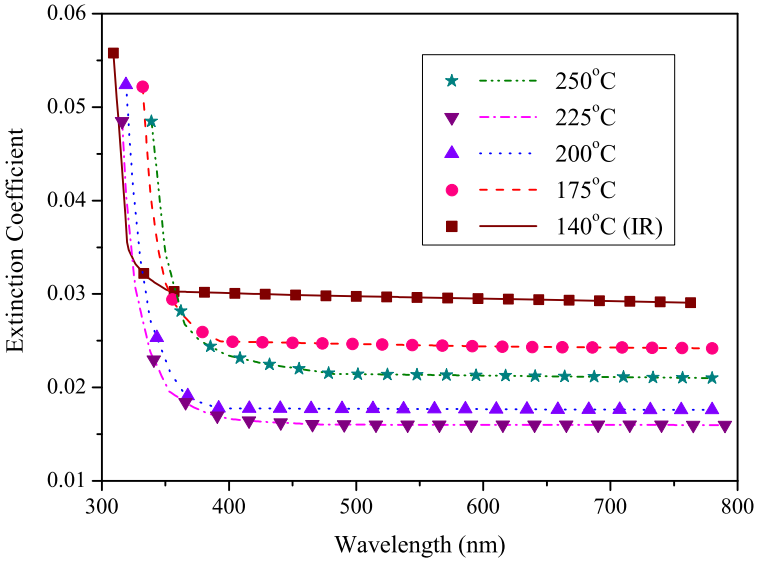

Figure 5. The extinction coefficients of ZnO nanocrystalline films dried at different temperatures and by IR radiation with annealing at 500°C.

extrapolating the straight line portion of this plot to the energy axis. E_g is the photon energy at the point where $(\alpha h\upsilon)^2$ is zero. The energy band gap increases from 3.20 to 3.35 eV when drying temperature changes from 140 (IR radiation) to 225°C and then decreases to 3.27 eV for 250°C drying temperature. The blue-shift of the optical band gap of ZnO

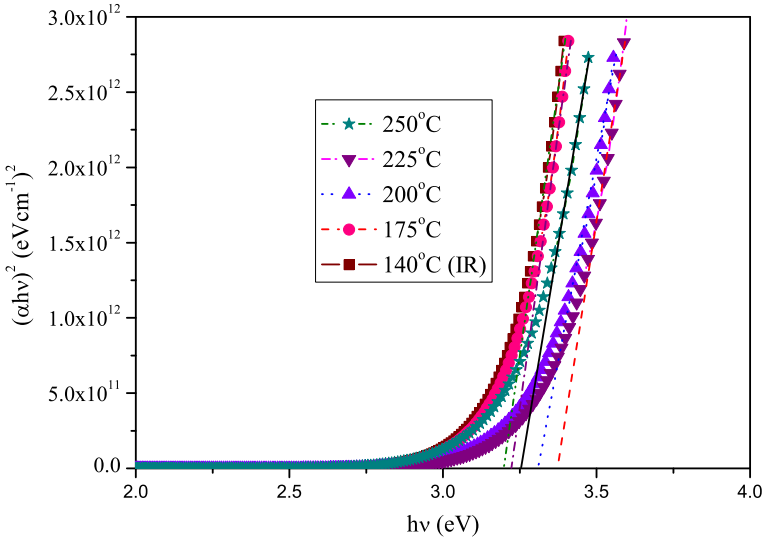

Figure 6. The optical band gap of ZnO nanocrystalline films dried at different temperatures and by IR radiation with annealing at 500°C.

nanocrystalline films can be attributed to the increase of the carrier concentration due to increase of oxygen vacancy with increase in drying temperature up to 240°C that blocks the lowest states in the conduction band (well known as the Burstein–Moss effect) [26]. In addition, the crystallization quality of ZnO film is improved and the stoichiometry and defect number decrease when drying temperature increases up to 240°C. When the drying temperature exceeds 240°C, the preferred crystal growth is distributed. This can result in an evident red-shift of the optical band gap with increase in drying temperature from 225 to 250°C. We should emphasis that this behaviour is a result of drying process of wet films which is different from the annealing process of dried films because a lot of substances vapourize during the drying process of wet films whereas in annealing process, the dried films try to rearrange themselves and the evaporation of substances is low.

Figure 7 shows the photoluminescence (PL) spectra of the ZnO nanocrystalline films dried at different temperatures and by IR radiation then annealed at 500°C for 30 min. There exist two emission peaks located about 370 and 410 nm [27], which correspond to the band-to-band transition [28,29]. The intensities of both UV emission peaks increase gradually when the drying temperature increases from 100 to 225°C and then decreases at 250°C. A broad band-to-band transition peak at about 400 nm was observed for sample dried at 250°C. It is proposed that the broadening of band-to-band transition peak is related to the antisite defects and roughness of surface (as found in AFM) of the films [30]. The results are in agreement with XRD analysis. The increased intensity of UV emission depends on the grain size and crystal orientation. In this study, the grain size, ZnO (0 0 2) diffraction intensity, and UV intensity increase by increasing the drying temperature up to 225°C. The grain size increases from 23 to 48 nm by increasing the drying temperature

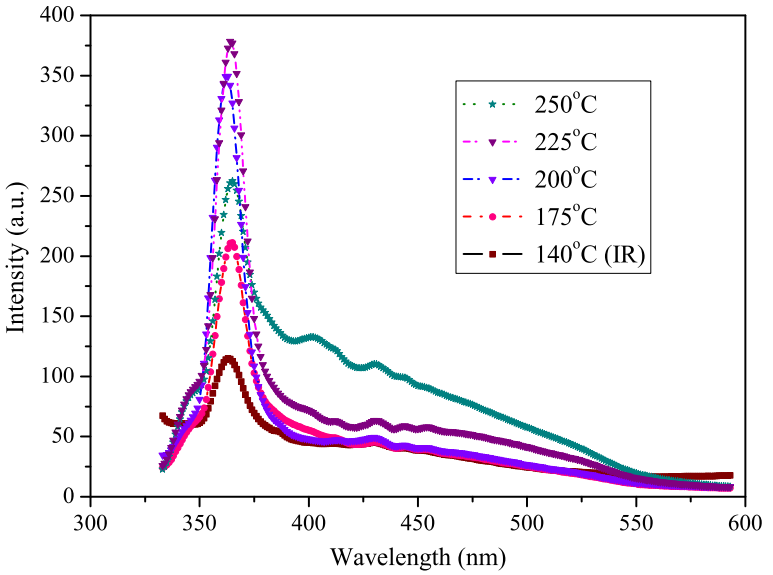

Figure 7. Photoluminescence spectra of the ZnO nanocrystalline films dried at different temperatures and by IR radiation with annealing at 500°C.

from 140 (IR radiation) to 225°C and decreases from 48 to 35 nm when the drying temperature increases from 225 to 250°C. The decrease in grain size of the sample dried at 250°C is due to reduction of thickness of the film that prevents the increase of the grain size and growth of the crystal. It should be noted that the PL spectra very much closely agreed well with the results of transmittance spectra. This is confirmed with the result of the XRD and transmittance as shown in figures 2 and 3. The PL results show that the characteristics of the ZnO thin films depend on the drying temperature.

Figure 8 shows the AFM images of ZnO nanocrystalline films dried at different temperatures in an oven and by IR radiation for 20 min, then annealed at 500°C for 30 min. We can see that increase of the drying temperature causes ZnO films to have smoother and denser surface morphology. There are some small pores in the sample dried at 200°C. Big punctures can be found in the samples dried at 175°C and by IR radiation. The high drying temperature causes decomposition of the zinc copolymers in precursor films and leaves some small pores in the films. These pores will be filled by new precursor solution in the next coating process, which makes the films denser. When the precursor films are dried at low temperature, the copolymers cannot decompose completely during drying process. The copolymers will combust during annealing treatment and big punctures are formed in the ZnO thin films.

Table 1 gives the drying conditions, roughness, grain size, thickness, refractive index at 550 nm, extinction coefficient at 550 nm, and optical band gap energy values of ZnO

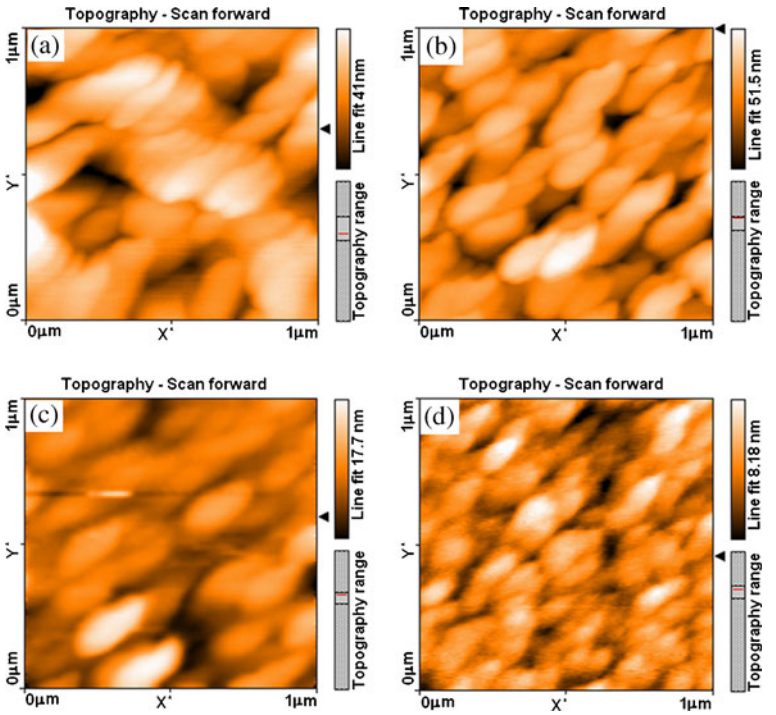

Figure 8. AFM photographs for surfaces of the ZnO nanocrystalline films dried at (**a**) IR radiation, (**b**) 175°C, (**c**) 200°C, (**d**) 250°C and annealing at 500°C for 30 min.

Table 1. Roughness, grain size, thickness, refractive index, extinction coefficient and band gap of ZnO nanocrystalline films prepared in different drying conditions.

Sample dried by	IR	175°C	200°C	225°C	250°C
Roughness (nm)	38.5	30.2	18.5	5.9	16
Grain size (nm)	23	28	39	48	35
Thickness (nm)	128	120	113	105	93
Refractive index	1.87	1.84	1.71	1.69	1.78
Extinction coefficient	0.029	0.024	0.018	0.016	0.021
Band gap (eV)	3.20	3.23	3.33	3.37	3.26

nanofilms. The changes in the optical constants of ZnO nanocrystalline films with the change in film thickness can be attributed to the changes in the grain size as discussed earlier. This means that the drying temperature and drying method affect the crystallinity, morphology and optical properties of ZnO nanocrystalline films.

4. Conclusion

ZnO nanocrystalline thin films were prepared by sol–gel method using dip coating technique and dried at different drying conditions. The optical, morphological, and structural properties of ZnO nanocrystalline films have been related to the drying conditions. The crystallinity of ZnO nanocrystalline films was enhanced by increasing the drying temperature up to 225°C and was decreased at 250°C. The film dried at 225°C had a highly preferred *c*-axis orientation along (0 0 2) plane. The optical transmittance of ZnO nanocrystalline films dried at 225°C has been improved while its refractive index and extinction coefficient have been reduced. The results in this study closely agreed with the results of ref. [19] with an exception for the sample dried at 250°C that can be related to use of different solvents for the production of sol.

Acknowledgements

The authors gratefully acknowledge Chemistry Department, The University of Guilan, for XRD and IR analysis and Chemistry Department, Razi University, for providing PL spectroscopy.

References

[1] H Y Bae and G M Cho, *Sens. Actuators* **B55**, 47 (1999)
[2] A Trinchi, Y X Li, W Wlodarski, S Kaciulis, L Pandolfi, S P Russo, J Duplessis and S Viticoli, *Sens. Actuators* **A108**, 263 (2003)
[3] Z C Jin, I Hamberg, C G Granqvist, B E Sernelius and K F Berggren, *Thin Solid Films* **164** 1945 (1989)
[4] Y Natsume, H Sakata, T Hirayama and H Yanagida, *J. Appl. Phys.* **72**, 4203 (1992)

[5] J M Biana, X M Li, X D Gao, W D Yu and L d Chen, *Appl. Phys. Lett.* **84**, 541 (2004)
[6] W Shen, Y Zhao and C Zhang, *Thin Solid Films* **483**, 352 (2005)
[7] J E Jaffe, J A Snyder, Z Lin and A C Hess, *Phys. Rev*. **B62**, 1660 (2000)
[8] Z K Tang, G K L Wong, P Yu, M Kawasaki, A Ohtomo, H Koinuma and Y Segawa, *Appl. Phys. Lett.* **72**, 3270 (1998)
[9] L Znaidi, G J A A Soler Illia, S Benyahia, C Sanchez and A V Kanaev, *Thin Solid Films* **428**, 257 (2003)
[10] Parmod Sagar, P K Shishodia, R M Mehra, H Okada, Akihiro Wakahara and Akira Yoshida, *J. Lumin.* **126**, 800 (2007)
[11] S W Xue, X T Zu, W L Zhou, H X Deng, X Xiang, L Zhang and H Deng, *J. Alloys Compounds* **448**, 21 (2008)
[12] S Hwangbo, Y Lee and K Hwang, *Ceram. Int.* **34**, 1237 (2008)
[13] S Mandal, M L N Goswami, K Das, A Dhar and S K Ray, *Thin Solid Films* **516**, 8702 (2008)
[14] H Cheng, C Chen, C Tsay and J Leu, *J. Alloys Compounds* **475**, 46 (2009)
[15] E G Brigin, I Chambouleyron, J M Martinez and S D Ventura, *Appl. Numer. Math.* **47**, 109 (2003)
[16] M Mulato, I Chambouleyron, E G Birgin and J M Martinez, *Appl. Phys. Lett.* **77**, 2133 (2000)
[17] I Chambouleyron, S D Ventura, E G Birgin and J M Martinez, *J. Appl. Phys.* **92**, 3092 (2002)
[18] X L Cheng, H Zhao, L H Huo and S Gao, *Sens. Actuators* **B102**, 248 (2004)
[19] H Li, J Y Wang, H Liu, C H Yang, H Y Xu, X Li and H M Cui, *Vacuum* **77**, 57 (2004)
[20] S Bandyopadhyay, G K Paul, R Roy, S K Sen and S Sen, *Mater. Chem. Phys.* **74**, 83 (2002)
[21] JCPDS-International Center for Diffraction Data, PCPDFWIN **6.0**, 05 (2000)
[22] M Ohyama, H Kozuka and T Yoko, *Thin Solid Films* **306**, 78 (1997)
[23] D Bao, H Gu and A Kuang, *Thin Solid Films* **312**, 37 (1998)
[24] M Wang, H Wang, W Chen, Y Chui and L Wang, *Mater. Chem. Phys.* **97**, 219 (2006)
[25] S A Mahmoud, A A Akl, H Kamal and K Abdel-Hady, *Physica* **B311**, 366 (2002)
[26] E Burstein, *Phys. Rev*. **93**, 632 (1954)
[27] H Jung, C Z Lu, Y Wang and C Son, *J. Korean Phys. Soc.* **45**, 959 (2004)
[28] G Srinivasan and J Kumar, *Cryst. Res. Technol.* **41**, 893 (2006)
[29] P T Hsieh, Y C Chen, K S Kao, M S Lee and C C Cheng, *J. Eur. Ceram. Soc.* **27**, 3815 (2007)
[30] F E Ghodsi and H Absalan, *Acta Phys. Polon.* **A118**, 659 (2010)